DOT/FAA/TC-14/52

Federal Aviation Administration
William J. Hughes Technical Center
Aviation Research Division
Atlantic City International Airport
New Jersey 08405

Nondestructive Inspection Research of Composite Materials Used on the Commercial Fleet: Infrared Imaging for Defect Detection in Aircraft Structures Using Chaotic and Broadband Sound Excitation

December 2015

Final Report

This document is available to the U.S. public through the National Technical Information Services (NTIS), Springfield, Virginia 22161.

This document is also available from the Federal Aviation Administration William J. Hughes Technical Center at actlibrary.tc.faa.gov.

U.S. Department of Transportation
Federal Aviation Administration

NOTICE

This document is disseminated under the sponsorship of the U.S. Department of Transportation in the interest of information exchange. The U.S. Government assumes no liability for the contents or use thereof. The U.S. Government does not endorse products or manufacturers. Trade or manufacturers' names appear herein solely because they are considered essential to the objective of this report. The findings and conclusions in this report are those of the author(s) and do not necessarily represent the views of the funding agency. This document does not constitute FAA policy. Consult the FAA sponsoring organization listed on the Technical Documentation page as to its use.

This report is available at the Federal Aviation Administration William J. Hughes Technical Center's Full-Text Technical Reports page: actlibrary.tc.faa.gov in Adobe Acrobat portable document format (PDF).

Technical Report Documentation Page

1. Report No.	2. Government Accession No.	3. Recipient's Catalog No.
DOT/FAA/TC-14/52		

4. Title and Subtitle	5. Report Date
NONDESTRUCTIVE INSPECTION RESEARCH OF COMPOSITE MATERIALS USED ON THE COMMERCIAL FLEET: INFRARED IMAGING FOR DEFECT DETECTION IN AIRCRAFT STRUCTURES USING CHAOTIC AND BROADBAND SOUND EXCITATION	December 2015
	6. Performing Organization Code

7. Author(s)	8. Performing Organization Report No.
Xiaoyan Han	

9. Performing Organization Name and Address	10. Work Unit No. (TRAIS)
Wayne State University Department of Electrical and Computer Engineering College of Engineering 5050 Anthony Wayne Dr., #3123 Detroit, MI 48202	11. Contract or Grant No. DTFACT-08-C-00043

12. Sponsoring Agency Name and Address	13. Type of Report and Period Covered
U.S. Department of Transportation Federal Aviation Administration Air Traffic Organization NextGen & Operations Planning Office of Research and Technology Development Washington, DC 20591	Final Report 1/28/2009 – 8/31/2013
	14. Sponsoring Agency Code

15. Supplementary Notes

The Federal Aviation Administration William J. Hughes Aviation Research Division COR was David Galella.

16. Abstract

This report documents the successful extension of Sonic infrared (IR) imaging technology to the inspection of widespread impact damage in composite aircraft structures. The technology detects delaminations, disbonds, and cracks in the composite skin by injecting low frequency ultrasound into the structure and then using an IR video camera to image the defects through the frictional heating produced by the acoustic vibration of the defect surfaces. As reported here, Sonic IR is capable of detecting and imaging multiple defects in a 10- to 12-square foot area in just a few seconds, making it the fastest technique for inspecting composite aircraft structures for widespread impact damage as of this writing. This advanced capability was developed by Wayne State University in a systematic research effort that started with the investigation of the fundamental properties of low-frequency ultrasound in composite materials and structures. This work included both experiments on composite specimens and mathematical modeling to verify the reliability of computational models for composite structures. Experimental work included laboratory samples and a variety of aircraft specimens manufactured by two different original equipment manufacturers (OEMs). These OEM specimens included several different stringer structures, doublers, ply drop-off regions, etc., each containing defects produced by impacts and other unspecified methods. The Wayne State University research and development effort culminated with the design and demonstration of a prototype portable Sonic IR inspection system for composite aircraft. The prototype consists of a handheld ultrasonic source, tripod-mounted IR camera, two-wheeled dolly that carries the power supplies for the camera and ultrasonic source, and laptop computer that controls the system and stores the images. Each image acquired with the prototype can have a field of view of approximately 5 or 6 feet in width and takes only a few seconds to acquire. Depending on the location on the aircraft, moving to the next station could take as little as 1 minute; progress across the plane can be rapid. Sonic IR inspections of the OEM specimens with the prototype system, by both experienced operators and novices with approximately one hour of training, consistently showed the defects regardless of the experience of the operator.

17. Key Words	18. Distribution Statement
Non-destructive inspection, Composites, Sonic infrared, IR, Ultrasonic, Aerospace, Continued airworthiness	This document is available to the U.S. public through the National Technical Information Service (NTIS), Springfield, Virginia 22161. This document is also available from the Federal Aviation Administration William J. Hughes Technical Center at actlibrary.tc.faa.gov.

19. Security Classif. (of this report)	20. Security Classif. (of this page)	21. No. of Pages	22. Price
Unclassified	Unclassified	45	

ACKNOWLEDGEMENTS

This work was sponsored by the Federal Aviation Administration (FAA) William J. Hughes Technical Center under Contract Number DTFACT-08-C-00043, with Agency Contract Number 437-65061, and Wayne State University.

The Wayne State University infrared imaging group wishes to thank our FAA program managers David Galella and Paul Swindell for their valuable discussions, suggestions through phone calls, conference meetings, and on-site visits during the project period.

We also wish to thank our collaborators Mike Ashbaugh, Bob Barry at Bell Helicopter; the FAA Airworthiness Assurance NDI Validation Center at Sandia National Laboratories; Jeff Thompson at The Boeing Company; United Airlines; Dr. David Hsu; and Siemens Energy for their assistance during the project, including their having supplied valuable specimens.

TABLE OF CONTENTS

LIST OF FIGURES

LIST OF ACRONYMS

AANC	Airworthiness Assurance NDI Validation Center
CFC	Carbon fiber composite
FAA	Federal Aviation Administration
FEA	Finite element analysis
IR	Infrared
NDE	Nondestructive evaluation
OEM	Original equipment manufacturer
SDK	Software development kit

EXECUTIVE SUMMARY

Wayne State University has developed Sonic infrared (IR) imaging as a practical tool for inspection of widespread impact damage on composite aircraft, such as might occur in severe hailstorms. Prior to this work, Sonic IR technology development had been primarily for detection of cracks in metals, with an emphasis on aircraft structures and engines. Extending the technology to the inspection of composite aircraft was not a simple reapplication of the existing methods used by several original equipment manufacturers (OEMs) for detecting cracks in turbine engine components because composites have fundamentally different physical properties from metals such as aluminum, steel, and titanium. During a Sonic IR inspection, several hundred watts of acoustic power are injected into the aircraft structure for a fraction of a second. Carbon fiber composites (CFCs) have much lower thermal conductivities than metals, which immediately raised the question of possible material damage due to heating at the point of sound injection. In addition, CFCs have different acoustic properties from metals; the dependence of sound propagation on frequency, structure, and distance from the source are important considerations. For these reasons, this effort began with a fundamental study of the behavior of low-frequency ultrasound in composites and composite structures. This study used a two-pronged approach involving both mathematical modeling and laboratory experiments with composite panels of various sizes obtained from the Federal Aviation Administration (FAA) Airworthiness Assurance NDI Validation Center and elsewhere. Specific tests designed to address the issue of damage revealed the possibility of damage to the composite material under extreme levels of ultrasonic power density. Measures were taken to guarantee that these extreme levels would not occur with the prototype Sonic IR system described in this report. Another outcome of the study was that ultrasound of suitable frequencies can use stringers and other aircraft structures as acoustic waveguides resulting in the propagation of the sound far from the ultrasonic source. This allowed for a more rapid detection and imaging of multiple defects over wider areas as compared to any other imaging technology. The work progressed from the behavior of ultrasound in composites to a study of the interaction of ultrasonic sound with defects, both in mathematical models and real samples. Because this was intended to provide a background for understanding Sonic IR, which relies on thermal imaging, the focus was on the mechanisms by which ultrasound generates heat in defects. Wayne State University, with FAA assistance, obtained several simulated fuselage panels manufactured by two OEMs, some of which had surface areas as large as 12 square feet. The panels had a variety of different structural reinforcements, such as stringers and doublers; all had multiple defects introduced by impacts and other methods. These panels were used to demonstrate the effectiveness of the mobile prototype Sonic IR system designed by Wayne State University as part of this project. When operated either by experienced or inexperienced operators, this prototype system was shown to be able to acquire a single image covering an entire 6-foot-long panel. The image showed the multiple defects scattered across the panel reliably and reproducibly, with only seconds needed for the entire process. Sonic IR is now ready for demonstration on actual composite aircraft with widespread impact damage.

1. INTRODUCTION

1.1 BACKGROUND

Sonic infrared (IR) imaging, known by names such as Thermosonics, Acoustic Thermography, and Siemat, was patented by Wayne State University in 2001. The invention was motivated by the inability of Wayne State University's previously patented technology, thermal wave imaging, to detect vertical cracks in metals and ceramics. Both Sonic IR and thermal wave technologies involve active thermography, in which the object under inspection is activated by an external stimulus. In thermal wave imaging, the stimulus is a high-power light flash, which heats an area on the surface of the target uniformly, after which an IR video camera captures the cooling of the surface. Because both sides of a vertical crack are heated and cool identically, they are invisible in the thermal image. In Sonic IR, the stimulus is a pulse of high-power ultrasound, and the source of the heating is friction between the broken surfaces of the crack. As with thermal wave imaging, an IR video camera is used in Sonic IR, but instead of showing up as variations in brightness as in thermal wave images, defects appear bright against a dark background. Vertical cracks appear as bright lines. Because some preliminary experiments with Sonic IR on composites had indicated its ability to see kissing disbonds, and because there was a need for a method for conducting rapid inspections over wide areas of composite aircraft for possible impact disbonds like that which may occur as a result of a hailstorm, it was proposed that Sonic IR be investigated for composite inspection.

1.2 OVERVIEW OF SONIC IR TECHNOLOGY

The basic components of a Sonic IR system are an ultrasonic source, an IR video camera, and a control and display system. Ultrasound causes the surfaces of cracks and disbonds to rub against one another, causing heat by friction. The resulting local temperature rise is detected by the camera and used to produce images of the defects. To get sufficient ultrasonic power, sources that operate in a much lower frequency range than those that are used for ultrasonic imaging are required. Such sources are ordinarily used for ultrasonic welding of plastics and are commonly available in the 15–40 kHz frequency range. Their power ranges from as much as 3000 watts for a 15 kHz model to hundreds of watts for a 40 kHz model. Fortunately, Sonic IR on composites requires only a few hundred watts of power. Whatever the frequency or power level of the source, only a single ultrasonic pulse of less than one second duration is used to make a Sonic IR image. It is the shortness of the input pulse and speed of the IR imaging process that make Sonic IR inspection so fast. It is the large distance that low-frequency ultrasound propagates in the composite material that enables Sonic IR to cover wide areas in a single image.

Injecting ultrasound from a transducer into an external medium normally requires a coupling medium. The liquids and gels used in ultrasonic imaging tend to cavitate and blow out under high power levels. Therefore, Sonic IR uses a solid, but soft, coupling material. A variety of materials, such as leather, cardboard, and Teflon™, have been used. Early in the work in metals, the Wayne State University team discovered that the right combination of coupling material and applied pressure could cause the injected sound to change its frequency composition. Instead of the single frequency produced by the transducer, the spectrum of the sound became a combination of many frequencies, some lower than the transducer frequency, and many higher than that of the transducer. This type of sound was dubbed "acoustic chaos," and it proved to be

uncommonly effective in Sonic IR imaging of cracks in metals. Its application and evaluation in composites was a major focus in this research effort.

A Sonic IR inspection is completed using one of a variety of cameras, all differing in speed, sensitivity, and price. The cameras used in this project were specialized, high-end research cameras capable of high video frame rates. However, these high frame rates are not utilized for composite inspections. Composites have low thermal conductivities when compared to metals and therefore do not require rapid response times to catch thermal images before they diffuse away. The Wayne State University software intentionally slows down the frame rate of the cameras, effectively making them comparable to less expensive cameras.

Wayne State University wrote the software specifically for Sonic IR applications. It runs on a laptop computer and contains control elements for the camera (e.g., to direct the camera to acquire and store images). The software also contains image-processing elements, some of which are common to any image processing software package, and some that were invented specifically for Sonic IR by the Wayne State University team. On the few occasions when the Wayne State University software was compared head-to-head with software from other sources using the same samples and similar cameras, the Wayne State University software detected defects that the other software packages could not. This is believed to be due to those specific image-processing elements invented by the university's team.

2. OBJECTIVES

The general objective of this effort was to determine whether Sonic IR could be established as a viable method for inspection of composite structures, especially composite aircraft fuselages, for widespread damage. Methods such as ultrasonic imaging already existed for local inspections, such as might be necessary after accidental contact with ground support equipment, but no methods exist for rapid inspection of aircraft caught on the tarmac during a hailstorm. Accomplishing this required a series of intermediate objectives:

- Ultrasonic Damage Tolerance of Aircraft Composites—A systematic study of the effects of power level, transducer size, coupling material, and other variables was performed. Sonic IR involves injecting a few hundred watts of acoustic power through a small contact area on the surface of the aircraft. The question of establishing the damage tolerance of the composite material is therefore of primary importance.

- Effects of Defect Size and Depth—Obtain composite samples with defects of different sizes and depths to determine their detectability.

- Effects of Structure—Sound propagation in the vicinity of different support structures was investigated. Composite aircraft have many different substructures under the fuselage's outer skin. These stringers, doublers, and other substructures can vary considerably in their construction and may affect sound propagation differently. Of special interest is the distance that sound travels in composite structures. This affects the maximum range from the sound injection point to the furthest detectible defect.

- Optimization of Transducer Frequency—Establish which frequencies are best for use on composites. Commercially available high-power transducers are intended for welding soft plastics like polyethylene and designed to produce frequencies that are suitable for that purpose. These frequencies range from 15–40 kHz.

- Evaluation of Chaotic Sound in Composite Materials—Find suitable combinations of transducer frequencies and coupling materials to generate acoustic chaos in composites, and evaluate the resulting sound for Sonic IR imaging. When inspecting metallic parts, the Wayne State University team found that acoustic chaos was preferable to the single frequency normally produced by commercial transducers. Acoustic chaos is composed of many frequencies ranging from a few kHZ up to 100 kHZ, and is generated through the interaction of the transducer with the metal surface through a coupling material under certain conditions.

- Optimization of the Sound Injection Process for Each Type of Sound—Determine for each frequency, or combination of frequencies, the injection parameters associated with obtaining maximum energy transmission into the aircraft skin. These parameters include the nature of the coupling material; the pressure between the transducer and the coupling material; the length of the pulse; the contact area; and a comparison of rigidly mounted and handheld transducers.

- Design of Prototype Sonic IR Inspection System—Design a Sonic IR inspection system and demonstrate it to the Federal Aviation Administration (FAA). A Sonic IR system is useful for in-service aircraft inspection if it is easily movable and preferably applied to the aircraft with a handheld transducer for maneuvering about the plane. This system should cover the widest possible area in the shortest amount of time and be capable of finding multiple impact damage sites anywhere within its coverage area. In addition, the Sonic IR system should include suitable software for controlling the system and displaying and storing the images on a laptop computer

3. APPROACH

3.1 LABORATORY EXPERIMENTS

The ultrasonic sources used in the experiments were purchased from Branson Ultrasonics of Danbury, Connecticut, and were originally designed for welding plastics. The lowest frequency transducer was a 3.3 kW, 15 kHz bench-mounted unit that was used in some laboratory experiments designed to test damage tolerance. However, the transducer's weight and excessive power prohibited it from contention for the final system. Next up in frequency, and down in power, were several bench-mounted and handheld 20 kHz units. Finally, there were bench-mounted and handheld 30 kHz and 40 kHz units. Special attention was given to the 40 kHz sources because of the previous success of those units with metal aircraft engine disks. The experiments finally focused on the 20 kHz sources because that frequency seemed to propagate furthest in carbon fiber composites (CFCs). Several designs of handheld mounts for the Branson 20 kHz sources were tested, but the final choice was for an off-the-shelf design sold

by Branson. It was convenient to use, and its 500 watts of power was more than adequate for composite inspections. It was normally operated at only 200–300 watts.

Both of the cameras used throughout the experiments were FLIR SC6000s operating in the 3–5 micron, or "mid-wave," IR. The FLIR SC6000's high frame rate capability was not necessary for composite inspections, and the cameras were operated far below their standard frame rates. This resulted in smaller image file sizes that took up less space in the computer's memory but in no way diminished their effectiveness for Sonic IR. In effect, they were being used as if they were less expensive cameras.

To learn more about how far sound propagated; what the frequency content and power levels were; and details regarding other variables in all parts of the large original equipment manufacturer test panels, as many as six laser vibrometers were used simultaneously on different regions of the panels. The vibrometers were manufactured by Polytec, whose North American headquarters are located in Irvine, California. The vibrometers work by reflecting a coherent beam of laser light from the surface of the sample and measuring the vibration of the surface, a process similar to how police radar measures the speed of a car. These vibrometers all used the same time base, so acoustic waveforms could be compared on a point-by-point basis at exactly the same time. They were triggered by the same signal that triggers the acquisition of the images by the camera, so detailed comparisons of the acoustic waveforms and the time dependence of images of defects could also be made on the same time base.

A coupling medium was always present between the titanium horn of the ultrasonic transducer and the surface of the composite whenever sound was injected into a composite structure. The purpose of this couplant was to facilitate better contact between the horn and the surface by filling in any small air gaps due to irregularities in the surface of the composite material. The horn itself has a highly polished flat surface. The liquid and gel couplants used in ultrasonic imaging could not be used here because they cavitate at the acoustic power levels used in Sonic IR. In the earliest experiments, a doubled piece of duct tape (Nashua 357) was used as the couplant because it was the most successful in work with metals. A thin piece of fiber-reinforced Teflon™ was always placed between the duct tape and the surface of the composite material. The Teflon was used to guarantee that the actual contact to the composite was made with an inert material. It is available from Taconic, of Petersburgh, New York. Later experiments used a variety of couplants, such as leather, business card paper, and cardboard—all with the thin layer of Teflon touching the surface of the composite material.

Chaotic sound cannot be generated with these couplants alone. To generate acoustic chaos, Wayne State University used a thin metal disc, with a rim to prevent it from slipping out, between the ultrasonic horn and the couplant. The discs were made of several metals, including aluminum, steel, stainless steel, and titanium. Acoustic chaos is generated at the interface between the horn and the metal. The presence of chaos is easily detected by the sound it makes. The ears of almost all adult humans cannot hear the fundamental 20 kHz sound produced by the transducer in the prototype system. When only this frequency, or this frequency and its higher harmonics, is present, there is no audible sound. However, the chaotic sound produced by the same transducer contains frequencies both much higher and much lower than 20 kHz. These

lower frequencies combine to make an audible screech that is the unmistakable signature of acoustic chaos.

The control center of the system was a laptop computer. Two older Lenovo® laptops running Windows® XP and a Dell™ laptop running Windows 7 were used. The images were exported from the cameras with a gigabit Ethernet (GigE) connection. A GigE connection is required for any computer used in these inspections. The imaging software running in the two distinct operating systems is functionally the same, but the low-level code is different. It is a program that Wayne State University has been developing for decades and is specifically designed for thermal wave and Sonic IR imaging applications. It contains a fully functional image processor with the addition of special elements to satisfy the needs of these technologies. Contained within these special elements is software obtained from FLIR software development kits (SDKs) that enables the laptop to control the camera settings and to acquire images using specific parameters (e.g., number of frames, frame rate, etc.). An external box divides the trigger signal and sends it to the vibrometers and the camera when vibrometer experiments are needed.

Obtaining appropriate samples was challenging. Many small composite samples with manufactured defects can be found at the FAA Airworthiness Assurance NDI Validation Center (AANC), Iowa State University, Wichita State University, and elsewhere, but the defects in most of those samples are designed as ultrasonic targets. The defects included foreign matter, pull-tabs, and back-drilled holes that are visible to ultrasonics. However, these are not real defects; they do not have the characteristic broken surfaces in contact that are almost always present in real defects, such as impact damage in composites. The other difficulty associated with using these samples for Sonic IR development is that they are small. These samples were designed to test ultrasonic systems that make local measurements. Though none of these samples met the size, structure, or defects requirements for Sonic IR, they did help to develop an understanding of the type of sample that was needed to represent actual aircraft structure. A scanning system is needed for ultrasonic system inspections of large areas. Sonic IR does not require a scanner. It is intrinsically a wide-area method and, as a result, requires large samples, with real defects, for meaningful testing.

The problem of obtaining real defects was partially solved by several impact damage samples that are part of a larger set that was made for the AANC. These samples were still small, typically two feet square, but with controlled impacts that caused internal damage. It is believed that the Sonic IR inspection detected all of the defects, but this cannot be confirmed. The AANC chose to keep the details of the samples confidential.

One exception to the acquired small samples was a much-traveled Airbus sample, which was reported to represent a section of an Airbus A330 vertical stabilizer. It was approximately 64″ x 23″. It had four composite enhancement ribs or stringers running the length of the back and four small composite stiffeners placed between the stringers. This sample had several defects, two of which were reported to be kissing disbonds because they were repeatedly missed in inspections with a thermal wave system elsewhere. The kissing disbonds were partial disbonds between two of the stiffeners and the composite skin. An early Sonic IR image of these two disbonds—together with an ultrasonic image that also showed them to be disbonded and a thermal wave image that incorrectly showed them as bonded—can be found in figures A-3 and

A-4 in appendix A. This panel has since been inspected with many technologies at multiple locations, so it is possible that those disbonds are no longer kissing. In addition to this panel demonstrating Sonic IR's ability to detect the kissing disbonds, the panel also revealed that substructure was important in Sonic IR imaging. The sound in the panel used the rear surface ribs as the walls of a waveguide and was channeled between them along the entire length of the panel. This showed the importance of subsurface components when inspecting composite structures.

The effects of substructure were further revealed in experiments with two 2′ x 2′ panels that the FAA obtained from Bell Helicopter. These panels had rather elaborate structures, with some unsupported single skin, some skin with rear-surface doublers, and with either I-beam or hat-channel ribs on the rear. In addition, each had been subjected to a series of impacts that left internal damage with no obvious front surface indications.

The real breakthrough in samples occurred when the FAA had Bell Helicopter manufacture two large composite panels. The panels' design is similar to that of the two smaller Bell panels. They were manufactured specifically for evaluating Sonic IR as a detector of widespread impact damage in realistic composite structures. One of the panels is approximately 21″ x 60″, and the other is approximately 24″ x 72″. Each has a doubler running its entire length along the center of the panel, with two stringers also running the length of the panel. The composite stringers on the 60″ panel had a hat-channel design, whereas those on the 72″ panel had an I-beam shape. Each of the panels were subjected to 19 separate impacts of varying severity. The impacts were distributed over the panels at positions on the unsupported skin, over the doublers, and over the stringers to provide a wide distribution in placement and size of defects. Photographs, engineering drawings, and C-scan images of these and some other samples can be found in appendix A.

3.2 MODELING

The modeling work in this project was divided into two areas: analytical modeling and finite element modeling. The analytical modeling was also divided into two sub-areas: modeling of sound propagation in composite structures and modeling of the formation of images of defects. The modeling of sound propagation was primarily to provide an understanding of the heating patterns that were observed when sound was propagating between barriers, such as stringers and edges of samples. Aircraft have no edges, so it was important to understand which parts of the patterns were artifacts of the finite size of our samples and which could be expected to be seen on real aircraft. The modeling of image formation enabled the development of an algorithm to determine the depth of a defect from the time evolution of the image.

Finite element modeling was usually accomplished with a commercial software package called LS-DYNA. This program had its roots in software that was originally developed at Lawrence Livermore Lab. It enabled the computational modeling of the entire Sonic IR process from the vibration of the transducer, to the propagation of the sound in the sample, and finally to the eventual heating of the defect and its surroundings. When the appropriate conditions were inserted into the program, it was able to duplicate the transition from a pure frequency to acoustic chaos. These elaborate and time-consuming computations were facilitated by a

136-node computer cluster from PSSC Labs, of Lake Forest, California, that was available for exclusive use by Wayne State University's nondestructive evaluation (NDE) team.

3.3 PROTOTYPE DESIGN

The underlying philosophy of the design of the prototype system was portability/mobility. This meant decreasing weight and making the system as compact as possible. Heavy camera mounts and bulky transducer power supplies were ruled out. Most ultrasonic welders are capable of power levels of 1 kW or more, and the resulting power supply cabinets are both heavy and bulky. Such large power output is not only excessive for Sonic IR, it can also heat the composite material beyond its damage limits if full power is used. Fortunately, Branson has a 500 W, 20 kHz power supply that connects directly to a handheld transducer and accepts any of their regular 20 kHz horns. The power supply has a footprint that is smaller than a square foot and fits nicely on the bottom of a small, two-wheel dolly. In use, it seldom is required to produce more than 200–250 W of ultrasonic power. Stacked above the power supply on the dolly is a video monitor; above that is the laptop computer that controls the system. Lightweight cables run to the camera and handheld transducer. The camera is normally mounted on a tripod; though, to make it more compact, it can also be mounted on the same dolly as the power supplies and the computer. The video monitor displays a live image from the camera, and the Sonic IR images are displayed on the laptop screen. Though it is not a necessary part of the system, a video splitter is also mounted on the dolly so that lab demonstrations can use a remote monitor. The software on the laptop is Wayne State University's own image processing and camera control package.

In practice, two people run the prototype: one controls the system using the software on the laptop while the other presses the handheld transducer against the panel under inspection. The prototype could be modified for operation by a single person; however, this step, which would require modifying both the hardware and the software, has not yet been taken.

4. RESULTS

4.1 LABORATORY EXPERIMENTS

4.1.1 Investigation of Transducer Contact Force and Power Level for Damage Thresholds

The transducer contact force and power level were studied for possible damage thresholds for single inspections and repeated inspections at the same location. The contact force is one of the parameters that determines how much of the transducer's power is actually transmitted through the coupling material to the composite surface. Though the transducer was removed and replaced at the same spot between firings, this force and the transducer's power setting remained constant during each series of repeated tests. These tests were conducted using a bench-mounted transducer, with the force being transmitted through a calibrated strain gauge for repeatability of the force setting. The samples for these studies were provided and characterized for possible damage by the AANC both prior to and after the testing in the lab. Similar before-and-after testing was done in the lab at Wayne State University using its thermal wave system as an additional check for possible damage. The methodology for this testing is illustrated by the panel shown in figure 1. This sample is approximately 18″ x 26″. The panel was marked with a two-inch square grid, with the rows and columns given alphanumeric labels so that the point of

application of the ultrasound could be recorded. The red circle indicates area C3, where the transducer was to be placed in a series of tests.

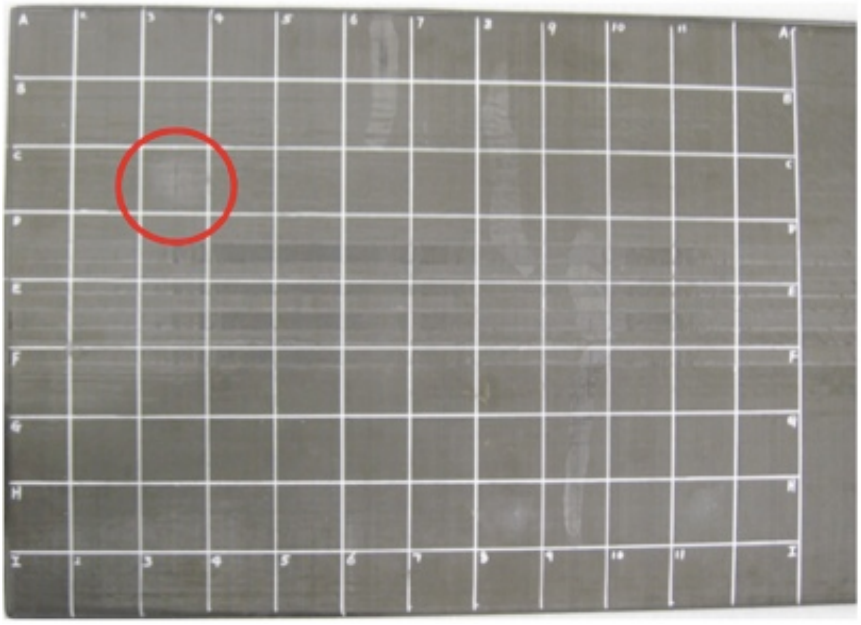

Figure 1. Photograph of the composite test panel with a red circle indicating square C3 (where the transducer was placed to inject ultrasonic pulses into the sample for a series of tests)

Figure 2 is a thermal wave image of the area in C3 made prior to any Sonic IR testing. This image served as a reference to determine any possible changes that might occur as a result of the injection of ultrasound into the material at this point. Note that there are some pre-existing areas of apparent damage in this sample. Most of these appeared as bright lines oriented along the direction of the tows in one of the plies, most likely the top ply. They likely are slightly unbonded edges of the tows. A larger disbonded area is indicated by the bright spot at the upper right section of the image. Like the bright lines, this is most likely a manufacturing defect.

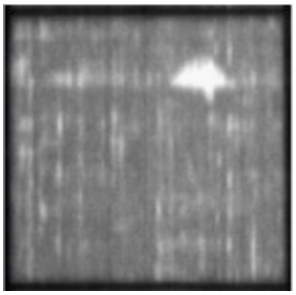

Figure 2. Thermal wave image taken before any test was done at the area C3

Subsequently, area C3 was subjected to multiple injections of ultrasound using the standard procedures and power levels as in Sonic IR imaging, but without the acquisition and storage of images. The sample was removed periodically and subjected to inspection with a thermal wave system for monitoring purposes. Figure 3 shows thermal wave images of C3 taken after 6, 36, and 66 repetitions of the sound injection process. These images are indistinguishable from the reference image in figure 2. No additional damage was ever found, though the number of applications of the sound at the same spot was far larger than ever would occur in actual inspections of an aircraft. Given the large area of an aircraft's exterior surface, the probability of the application of the transducer at exactly the same spot, even once, in repeated inspections is unlikely, so this test represents an exaggerated situation.

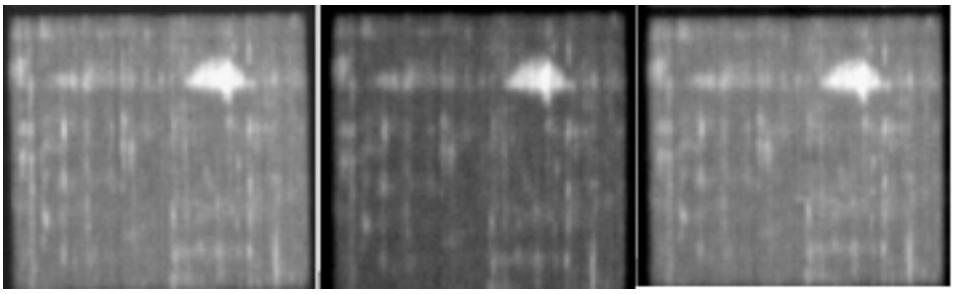

Figure 3. Thermal wave images of the region C3

Tests, such as the one described in this section, on the area C3 with varying ultrasonic power and applied force showed that, with power levels below 400 W and with typical coupling materials in place, no damage was caused by the Sonic IR inspections. These results were verified by post-Sonic IR inspections at AANC. However, with power levels approaching 1 kW, or with direct contact between a small-diameter transducer horn and the composite, it is possible to induce surface damage, especially to paint on the surface. The prototype system designed for this project avoids such problems by using a low-power, handheld transducer with a large diameter horn to reduce both the pressure on the surface and the power density delivered to it.

4.1.2 Elimination of Interference and Mode Patterns with Chaotic Sound

The CFCs differ from metals in that they attenuate sound rather strongly, increase in attenuation with increasing frequency. This has two effects: 1) a reduction in the distance that the sound travels in the composite and 2) dissipated energy appearing as heat in the material. In an aircraft

skin with subsurface structures such as stringers, the sound tends to reflect from the structures, creating complicated patterns in the intensity of the sound. The resulting uneven energy dissipation creates corresponding patterns in the temperature of the material, and these can serve to obscure the heating from defects in the Sonic IR images. Chaotic sound, with its multitude of frequencies, can be used to mitigate this effect. An example of this is shown in figure 4, in which an impact damage sample obtained from AANC is shown in two Sonic IR images—one made with a pure frequency and one made with chaotic sound. The difference in clarity of the images is dramatic. This sample has two damaged areas: 1) a larger one shaped like a human ear and 2) a much smaller one adjacent to it. In the pure-frequency image, the smaller defect is almost totally obscured and the details of the larger one are distorted nearly to the point of unrecognizability.

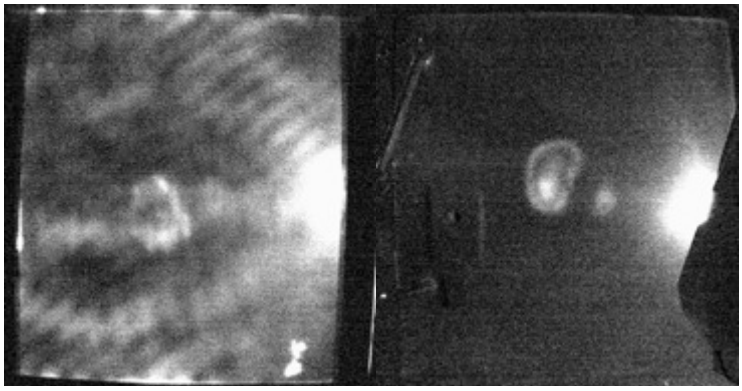

(a) (b)

Figure 4. Two Sonic IR images of impact damage in a composite sample from AANC ((a) was made with a 40 kHz frequency of sound and (b) with chaotic sound from the same source. The patterns on (a) would be different in detail if a different frequency was used, but they cannot be removed by changing the frequency.)

The bright spot on the right in each image in figure 4 is the area heated by the transducer. The artifacts of the patterned acoustic heating emanate from the location of the transducer in the single-frequency image. In the chaotic-sound image, the patterns appear to be totally absent. How does chaos do this? Figure 5 shows the actual acoustic spectra, or distribution of frequencies, in the two pulses used to make the images in figure 4. Note that the spectrum of the chaotic pulse contains many frequencies, both higher and lower than 40 kHz produced by the transducer, but with only a small amount of the transducer's original frequency still present. Chaotic sound consists of many closely spaced frequencies with the total acoustic energy distributed among them. Each of these frequencies by itself would create patterns like those in figure 4. However, these patterns are frequency-dependent, so the patterns from each of the frequencies in the chaotic case overlap, more or less randomly creating a uniform low-level background heating. The automatic gain control in the system then suppresses this uniform background to make it appear as if no patterns were generated.

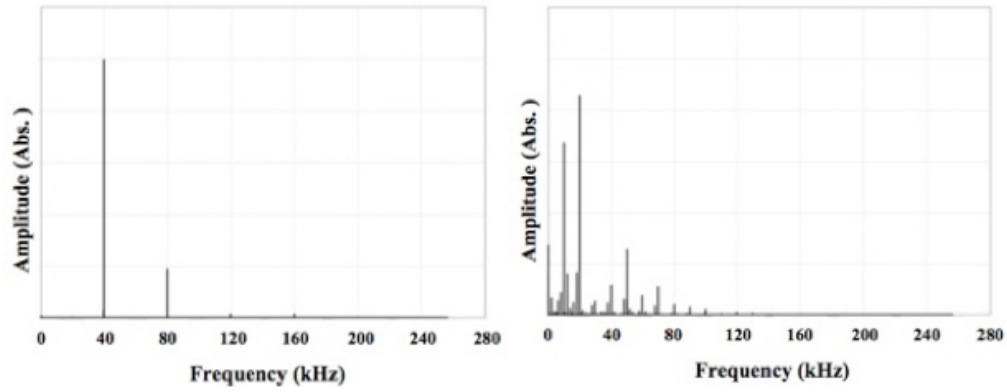

(a) (b)

Figure 5. The spectra of the sound pulses used to make the images in figure 4 ((a) is the 40 kHz frequency [also containing a little of the 2nd harmonic at 80 kHz] spectrum of the pulse that produced figure 4(a); (b) is the spectrum of the chaotic pulse that produced figure 4(b). These spectra are fast Fourier transforms of vibrational waveforms obtained directly from the sample itself using a laser vibrometer.)

Chaotic sound is not always the best choice for Sonic IR. Most of the frequencies in chaotic sound are higher than the driving frequency of the transducer (20 kHz in the Wayne State University prototype). The attenuation of ultrasound in CFCs increases rapidly with frequency. This means chaotic sound loses its higher frequencies quickly as it propagates and has less range and therefore a smaller area of coverage. For small areas, like the sample in figure 4, chaos is highly desirable. For surveying aircraft, in which wide-area coverage is important, it is probably better to use a single frequency and get a wider area into a single image. The area near the transducer will be somewhat obscured by interference patterns, but that area will also be partially blocked from the camera's view by the inspector holding the transducer. A transducer mount could be designed to avoid this, but that would greatly reduce the mobility of the system. Because of the speed of the handheld system and the ease of moving it to the next station, it is better to accept the patterns and pick up any blocked area in the next image.

4.1.3 Experiments With Smaller Samples

Bell Helicopter, with FAA assistance, manufactured two large-impact damage panels specifically for testing Sonic IR. The structure of these panels was based on two smaller 2′ x 2′ panels that were previously obtained from Bell. A photograph of the rear side of one of the smaller panels is shown in figure 6(a). This panel has two I-beam stringer-like reinforcements with doublers between them and the skin and a doubler running down the center. It had been subjected to eight impacts on the front side. Three of the impacts were over an I-beam, three were over the central doubler, and two were over the single skin. The front side was painted with glossy aircraft paint that was unmarked, suggesting it was painted after the impacts. Bell provided the ultrasonic time-of-flight image of the panel shown in figure 6(b). In the ultrasonic image, the doublers show as three vertical stripes. The damage done by the eight impacts shows as irregular dark blue spots. Compare figure 6 with the Sonic IR image of the same panel shown in figure 7. In the Sonic IR image, the impact damage shows as bright spots against a uniformly dark background. The edges of the doublers can just barely be seen as dark edges against the background heating

of the single skin in the image. The pattern of the bright spots clearly matches the locations of the damage shown in the ultrasonic image in figure 6.

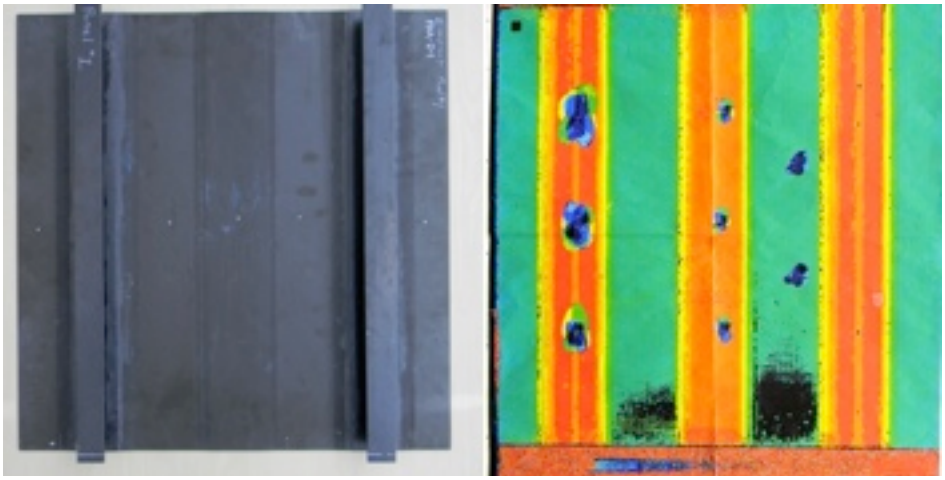

(a) (b)

Figure 6. The (a) photograph and (b) ultrasonic image of a 2′ x 2′ I-beam panel from Bell Helicopter ((a)is a photograph of the rear side of a 2′ x 2′ panel provided by Bell Helicopter showing the reinforcing I-beams and doublers; this panel was subjected to impacts from the front by Bell at eight different sites; (b) is Bell's time-of-flight ultrasonic image of the damage in the panel.)

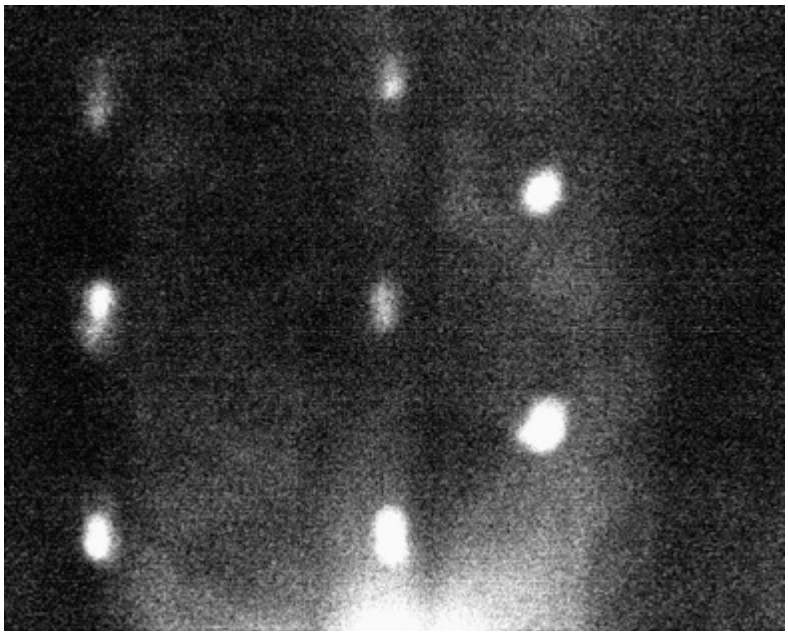

Figure 7. Sonic IR image of the panel shown in figure 6 (the damage at the eight impact sites is clearly visible; the transducer was placed at the bottom center over the doubler)

Bell also provided a second 2′ x 2′ panel of similar construction, except that the I-beam reinforcements were replaced by hat channels. Other than the "brims" of the hats, there was no extra skin thickness under the reinforcements. Therefore, the area within the channel was a narrow band of single unsupported skin. Knowledge of this difference in structure is important for Sonic IR imaging. Figure 8 shows a Sonic IR image of this hat channel sample made in exactly the same way as the Sonic IR image in figure 7, together with a small copy of the time-of-flight ultrasonic image from Bell. The pattern of the impacts is slightly different in this sample, but the most important difference is that, except for a faint indication of the defect nearest the transducer, the defects within the hat channel are not visible in the Sonic IR image. The five other defects are quite clear. The reason for the absence of the other defects is that the ultrasound has been mostly confined to the central region by the acoustic waveguide effect of the two hat beams. However, the narrow strip of single skin between the brims of the hat is also a waveguide. If the sound is injected into this strip (as shown in figure 9), the defects in that region appear as bright spots. The bottommost spot blends in with the heating from the transducer.

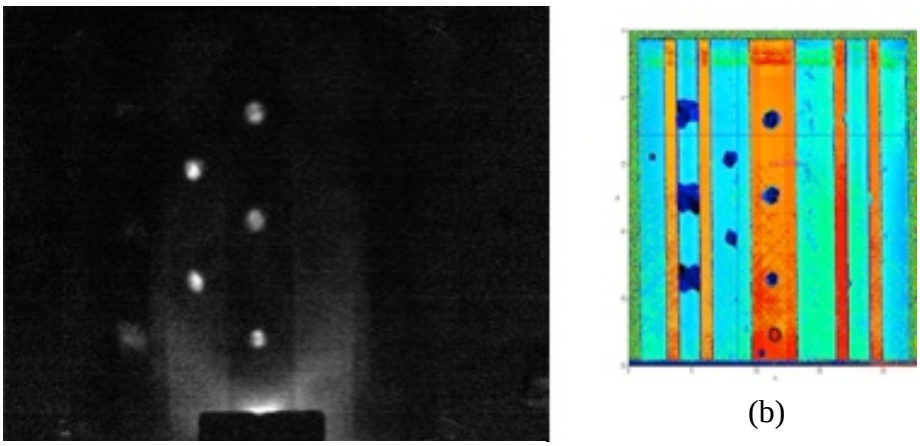

(a) (b)

Figure 8. The (a) Sonic IR and (b) ultrasonic images of 2′ x 2′ hat channel panel from Bell Helicopter ((a) is a Sonic IR image of a second 2′ x 2′ impact damage sample from Bell Helicopter with hat channels replacing the I-beam reinforcements seen in the sample in figure 6; (b) is a time-of-flight ultrasonic image, also from Bell, showing the damage from eight impacts. Note that, except for a faint image at the bottom of the channel, the three damage sites within the hat channel do not show in this Sonic IR image, which was made with the transducer placed at the bottom center of the panel.)

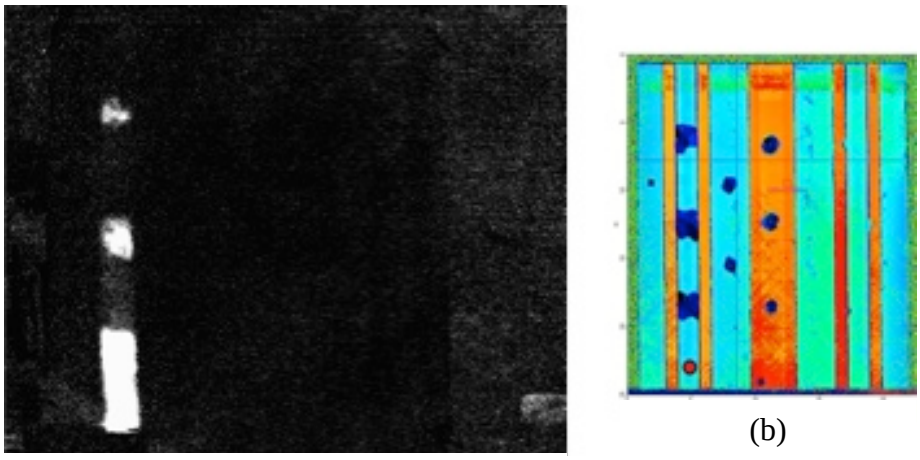

(a) (b)

Figure 9. The (a) Sonic IR and (b) ultrasonic images of 2′ x 2′ hat channel panel with the transducer over hat channel (a Sonic IR image of the same sample made with the transducer placed at the bottom end of the hat channel. This makes the damage within the channel clearly visible.)

Figures 8 and 9 show that structures under a composite aircraft skin can affect the propagation of sound and, therefore, must be taken into account in Sonic IR inspections. Obtaining samples with appropriate substructures was a major obstacle for this project, particularly obtaining samples with substructures that were also large enough to demonstrate Sonic IR's ability to find widespread damage. The first large sample with a structure that was available for testing was the

Airbus panel. This panel had longitudinal stringers, but only a few defects, and those appeared to have been deliberately introduced in its fabrication. Though it had no real defects, this panel did serve two purposes. First, it demonstrated that Sonic IR could detect kissing disbonds that were missed by other thermal methods. Second, it was the first sample to exhibit the acoustic waveguide effect, which is shown in figure 9 with the smaller hat channel sample. In the next section, this effect is also shown to occur in the large Bell Helicopter panels, which have many damage sites and in which one can see the ability of Sonic IR to detect and image widespread damage.

4.1.4 Experiments on Larger Samples

The Airbus sample, which was over 5′ long, was the first of the larger samples inspected by Sonic IR. The inspection occurred during a visit by the Wayne State University team to AANC in 2004. The kissing disbonds were first detected by a thermal method during this inspection, though they were already known as the result of previous ultrasonic scans. All of the disbonds in this sample appear to have been deliberately fabricated. A photograph and an engineering drawing of the sample can be found in appendix A. Well before any other large composite panels were available, the Airbus sample was used to show that it might be possible for Sonic IR to detect damage at relatively large distances from the ultrasonic source. This was accomplished with a variation of the familiar trick of demonstrating ultrasonic systems in undamaged samples by inserting ultrasonic targets like foreign materials into the samples. In this case, the inserted targets were steel washers bonded to the rear surface of the panel with a thick layer of glue. Coins or any other fairly massive flat object would do as well in place of the washers. When the panel vibrates, the inertia of a washer causes it to vibrate out of phase with the panel and, therefore, flex the glue. The heat dissipated in the glue then propagates to the front surface and simulates a defect. For the Airbus sample, a series of washers was placed along the centerline of the central channel, which was not blocked by stiffeners. This channel was selected because the stiffeners tend to reflect some of the sound back to the source and reduce its intensity further along a channel. After five washers were in place, a Sonic IR image was made with the transducer at one end of the panel. The locations of the washers lit up all the way to the other end, thereby demonstrating the possibility of imaging features at least 5′ from the source. This image is shown in figure 10.

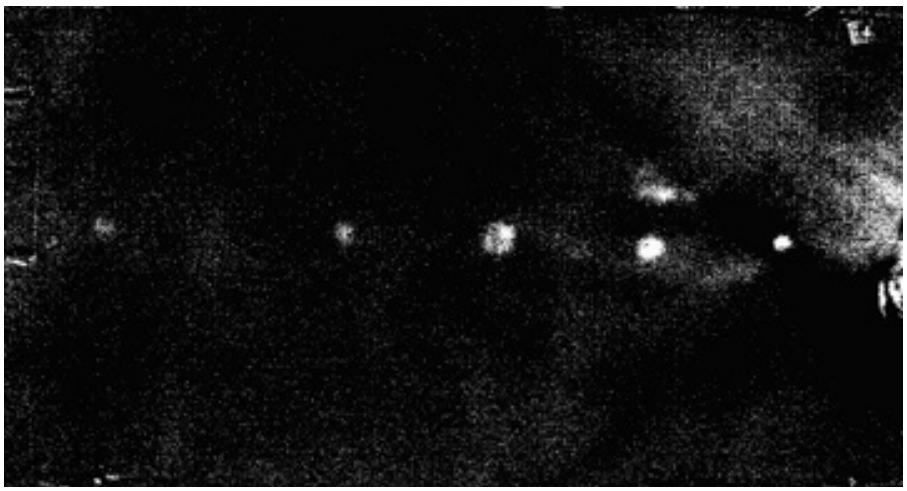

Figure 10. Sonic IR image of the five washers glued to the rear of the Airbus panel (the washers are not all the same size. The sound was inserted on the right end, just outside the edge of the image, and the furthest washer seen on the left was roughly 5′ from the source. The bright spot above the second washer from the right is one of the fabricated gaps between a stringer and the skin.)

The FAA arranged for Bell Helicopter to manufacture two larger panels and to have each of them impacted at 19 widely distributed points with a distribution of energies in the impacts. These impact energies were chosen so that they would cause internal damage but only barely visible surface damage. Almost none of the impacts could be detected visually, even in glancing light. This was in spite of the fact that the samples were painted with glossy white aircraft paint which would show the slightest surface dimple in such light. These panels were the principal targets during the final development of the prototype system, and the evaluation of that system with operators of different experience levels was the focus. Figure 11 is a typical Sonic IR image of one of these panels taken during the evaluation of the four different operators. This is the 5′ long hat channel panel; the image was made with Operator III holding the transducer. The only semi-critical part of the imaging operation is placing the transducer in an appropriate position and maintaining the face of the transducer's 1″ diameter horn flat against the panel for the less than 1-second duration of the acoustic pulse. The rest of the imaging is handled automatically by the software and is operator independent.

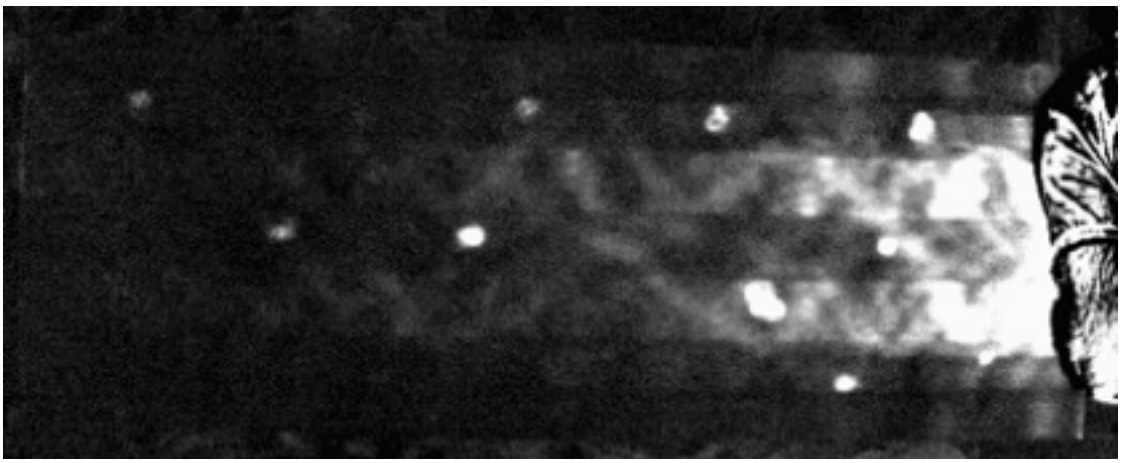

Figure 11. A 20 kHz single frequency Sonic IR image of the hat channel panel taken during evaluation of the performance of the four operators (the furthest defect seen in this image is roughly 5′ from the ultrasonic source on the right edge of the sample)

The operator in figure 11 was attempting to avoid blocking the view of the panel by standing off to the right. He had placed the transducer near the right edge of the panel. Some of the background patterns on the right are due to the effects of that edge, which would not be present in a real aircraft. This effect is explained in section 4.2. On a real aircraft, the patterns would not be so severe. Even with the patterns, defects can be seen quite close to the transducer. A time-of-flight ultrasonic image of this sample and the layout of all the impacts can be found in appendix A.

4.2 MODELING

4.2.1 Analytical Modeling

Analytical modeling, as opposed to purely computational modeling like finite element methods, has the advantage that the end product is an actual formula for the result, and knowledge exists as to exactly how the formula was derived. This means that the physical origins of the effects it predicts are exactly known. When computational modeling produces an effect, it is not always clear which details of the model caused the effect and, therefore, uncertainty exists about when and where the same effect might appear again. In addition, finite element models tend to be computationally intensive and require large amounts of computer time, preferably on large-scale parallel-processing machines. However, finite element methods can tackle problems that are beyond the ability of even the cleverest brains to solve analytically. Ultimately, both methods are needed.

The use of analytical modeling for Sonic IR in composites can be illustrated by certain features shown in figure 12. This is a Sonic IR image of a honeycomb-core sample that is approximately 1.5′ square. It has a variety of implanted ultrasonic-target type “defects,” many of which show up in the image. However, it appears from the background heating pattern that the sound is propagating out from the transducer horn in a series of beams, rather than spreading out uniformly in all directions.

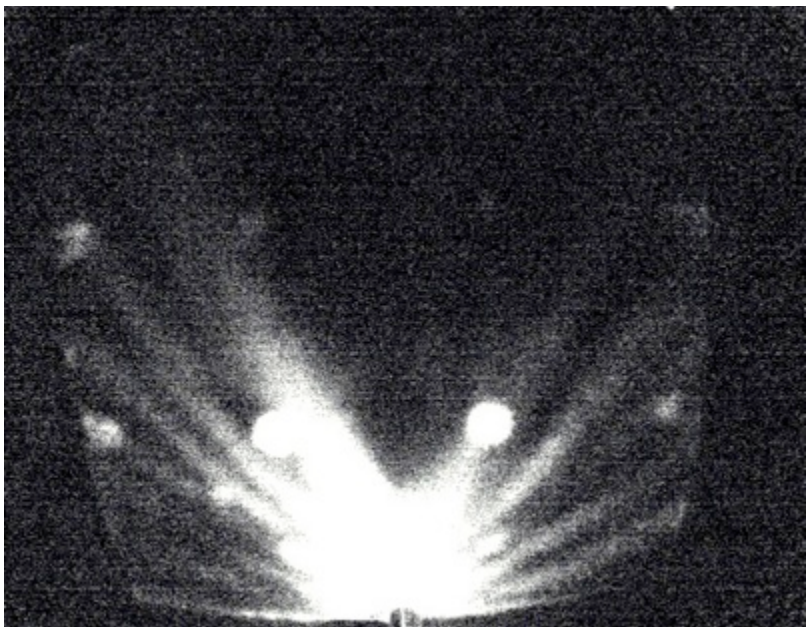

Figure 12. Sonic IR image of a 1.5′ square honeycomb panel showing implanted objects and sound appearing to propagate in a spray of narrow beams

The results of an analytical calculation that shows the same "beam" effect as in figure 12 are shown in figure 13. The calculation shown in figure 13 contains only the essential cause of the beams in the experimental image. In the calculation, the sound is allowed to reflect from the bottom edge of the sample, but not from any other edges. In the experimental image, the sound has diminished before it reaches the other edges, so what would happen there is irrelevant. For simplicity, this damping of the sound intensity was not included in the calculation. The effect of the edge reflection is that the reflected sound interferes with the directly emitted sound to produce a series of bands of high and low intensity. The number and intensity of the bands depends on the distance of the transducer from the edge. This distance and the other parameters of the panel were chosen to reproduce as accurately as possible the same number of beams as in the experimental image. This effect is the explanation for the patterns near the transducer in figure 11. However, in that image, the beams are also reflected from the stringers, so the pattern is more complicated.

Figure 13. The result of an analytical calculation of the effect of the reflection of sound from the edge of a sample (this effect was seen experimentally in figure 12)

Another example of the use of analytical modeling is the derivation of equations that describe the time dependence of Sonic IR images in composite materials. It is not apparent from any of the single images shown in this report, but in the video output of the camera, the images of deeper defects appear later in time than the images of shallower defects. This is because it takes longer for the heat generated at deeper defects to reach the surface of the material. If properties of the composite material—such as thermal conductivity or density—are known, this time can be calculated for a planar defect at any given depth. This procedure can also be reversed; the depth of a defect can be calculated from the knowledge of the time of its appearance in the image. This is shown in figure 14, which is a plot of calculated and measured times and depths of defects in some CFC samples obtained from AANC. The agreement is remarkably good and shows that this analytical method could be used to design a software routine to measure defect depths. With this addition, the Wayne State University Sonic IR system could measure not only the location and size of a defect but also its depth.

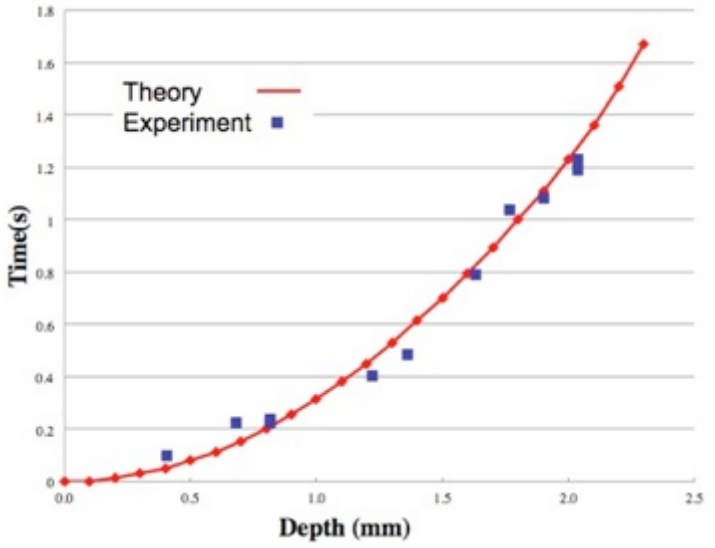

Figure 14. Experimental results vs. results from analytical calculations on depth determination from measured image appearance times

4.2.2 Finite Element Modeling

Finite element models tend to be computationally intensive and require large amounts of computing time, even on fast computers. Still, finite element models are useful because they can solve problems that are out of the range of any analytical calculation. The advantage of finite element analysis (FEA) is shown in figure 15, which shows a greatly exaggerated picture of the acoustical deformations of a composite panel with a centrally located square delamination when sound is injected. This model was important because it yielded an unexpected result. It showed that under the ultrasonic vibration, the surfaces of the disbond separated. This appeared as the simultaneous outward motion of both the front and rear surfaces of the sample directly over the disbond. A side view of the surfaces taken from the FEA file shows both sides bulging at the same time as indicated in figure 16. This result is important because no friction can occur between the defect surfaces during the time that they are separated.

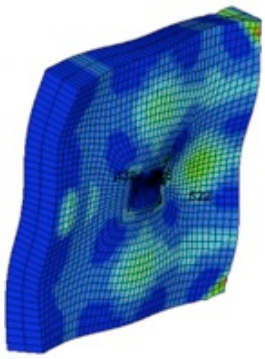

Figure 15. Finite element model of acoustic motion in the composite panel with a square defect

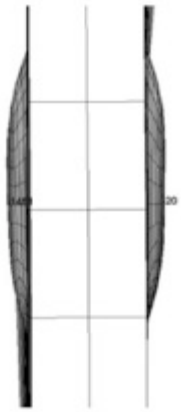

Figure 16. Side view of the out of plane motion from FEA

The FEA results shown in figures 15 and 16 were later confirmed experimentally through the use of a pair of laser vibrometers placed on opposite sides of a sample containing a central disbond, much like the one in the FEA model.

4.3 PROTOTYPE TESTING

The primary goal of the Sonic IR project on composites was the design of a prototype system that could be used in a hangar environment. The secondary goal of Sonic IR was its use outside on the tarmac. This meant that it had to be easily transportable, lightweight, and simple to operate, even by relatively untrained personnel. The intention was to fill a hole in existing NDE technology—namely, the lack of any system that could do rapid, wide-area inspection of composite aircraft and find hidden disbonds and delaminations within the composite skin.

The laboratory Sonic IR system used at the beginning of the project included a rack-mounted computer, transducer housings that were bolted to a table, and heavy, large-diameter cables that connected the camera to an electronic control unit that was mounted in the same rack as the computer, which, in turn, was connected to the computer. This system was neither portable nor mobile.

A Sonic IR system consists of three basic parts: an ultrasonic transducer, an IR camera, and a computer. Because the transducer has to contact the surface of the aircraft to inject the sound, and the camera has to stand off to take the pictures, it was not feasible to incorporate all three parts into a single small package that could be carried around the hangar. Therefore, mobility was chosen over portability. Some of the system is carried on a two-wheeled dolly.

The first change from the laboratory system was to use a new camera that had the ability to send images directly to the computer through an Ethernet cable. This eliminated the heavy camera cable and the electronic control unit. A consequence of this change was the need to rewrite the camera control software so that the computer controlled the camera, rather than the electronic control unit. The software rewrite was delayed while waiting for FLIR to release a new, camera-specific SDK.

The delay time was devoted to using the laboratory system on the composite samples that were available and by testing a variety of handheld housings for the array of frequency transducers that were already available in the lab. These housings were designed and built at Wayne State University or were commercial housings, including some that were modified at Wayne State University. These experiments led to a decision to select a 20 kHz Branson handheld unit and the commercial housings as standard. The 20 kHz frequency was chosen because it has superior propagation range compared to 30 kHz or 40 kHz. The commercial housing was chosen because it worked well and was available off the shelf. A Branson 500 W power supply was chosen to power the unit because of its low weight and small size, and experimentation showed that there was no need for power greater than a few hundred watts. A more powerful supply increases the chance of human error, such as a forgetful operator turning the power all the way up, which can cause damage to the section. One-inch diameter ultrasonic horns on the transducers were chosen over the smaller 1/2-inch or 3/4-inch horns usually sold with the Branson handheld housing. This was to reduce the power density per unit area on the aircraft and, therefore, further reduce the possibility of damage. This change had the added advantage that it made it easier for the operator to hold the horn flat against the composite surface and further reduced any tendency for the system to be operator-sensitive.

A photograph of the Branson handheld unit is shown in figure 17. A photograph of the prototype in use taken during evaluation of various operators is shown in figure 18. In this photograph, the two-wheeled dolly carrying the laptop computer and two power supplies (one in use and one spare) is shown in the foreground. The operator holding the Branson handheld transducer unit is seen about to inject the sound into one of the Bell Helicopter panels behind, and slightly to the right, of the dolly. A student is seen ready to click the mouse to fire the transducer and start the image acquisition. Below the computer is a video display showing a real-time image from the camera. The final Sonic IR images appear on the computer screen and are stored. The camera is visible on a tripod in the background. It can also be mounted on an upright post on the side of the dolly for direct operation, therefore reducing the number of units that must be moved to the next inspection station. The Branson transducer unit can also be hung on a hook on the dolly to facilitate ease in moving the system.

Figure 17. Photograph of the handheld 20 kHz Branson unit with the 1″ diameter horn attached

Figure 18. The prototype system being tested in the lab (a two-wheeled dolly carries the power supply for the transducer, a video monitor, and the computer that controls the system. A second, newer power supply was being stored on the dolly for later testing. The operator in the background is holding the handheld transducer against a large aircraft composite panel, and the IR camera is mounted on a tripod in the background. For more compactness, the camera can also be mounted on the dolly.)

The evaluation of the prototype was completed by four sets of operators running the system sequentially. These operators had different levels of experience—from novice students to those who had operated the system hundreds of times. Because the system is intended for wide-area inspections, the testing was completed using the two largest panels from Bell Helicopter as targets and with the camera focused to include an entire panel in each shot. The panels were mounted upright, with the stringers running horizontally as they would in an actual aircraft. The stringers were attached to posts simulating frames behind the sample so that the composite skin was supported only by the stringers, again simulating the situation in an actual aircraft. The criteria for evaluating the results were the number and brightness of the images of the individual impact sites. A brief training period was used to give each operator a chance to learn how much force to apply to the transducer and to learn how to keep the face of the ultrasonic horn flat against the surface of the panel. The different operators were then compared with each other to determine the degree of operator independence that could be expected from the system. Photographs of different operators using the system during the evaluation process can be found in appendix A. The results of the evaluations are presented in appendix B.

5. DISCUSSION

The development of Sonic IR imaging coincided with the emergence of the new generation of composite aircraft. After exposure in a severe hailstorm, aluminum aircraft can quickly be visually inspected for surface dents, and if no significant impact damage is detected, put back into service. The same cannot be said for aircraft with CFC skins, which can suffer severe internal damage from impacts without exhibiting any obvious surface damage. There is a need for a new method of performing a quick survey of a composite aircraft after an event like a hailstorm. Ultrasonic systems are good at finding impact damage in composites, but only on a very small area unless a cumbersome and time-consuming scanning system is used. Thermal wave imaging can also find impact damage on small areas and is faster than ultrasonics, but it requires multiple images to cover larger areas and is known to miss kissing disbonds (see appendix A, figures A-3–A-5). However, Sonic IR can find impact damage in an area of 12 square feet in just a few seconds and can also find kissing disbonds. With the mobility of the Sonic IR prototype developed in this project, it should take only a few minutes to move between inspection stations. This time was estimated by setting up the two large Bell Helicopter panels a short distance from each other, making an image of one, and then moving to the other panel and making a second image. Most of the time was spent adjusting and focusing the camera so that the entire panel was included in the picture. The time it would take to inspect an entire aircraft fuselage under realistic conditions is difficult to estimate because large-scale composite testbeds are rare, and none have yet been made available for evaluating the prototype.

No NDE system can do everything. Sonic IR can be used for local inspections if, for example, a forklift accidentally bumps a plane, but is better utilized when used for fast, wide-area inspections. It is the fastest inspection system for surveying an aircraft for widespread impact damage as of this writing. The Wayne State University prototype was designed for easy mobility both within hangars and outside on the tarmac. It has been successfully tested in the lab on composite panels manufactured by Bell Helicopter and Boeing Commercial Airplanes to ensure that the structures tested were manufactured under identical conditions to those used in current production aircraft (note that a non-disclosure agreement prevents our showing Boeing samples here). The technology is sufficiently mature that it should now undergo large-scale testing on an actual aircraft.

6. CONCLUSIONS

An understanding of the fundamental processes involved in the production of heat in composite defects has been achieved on both a theoretical and an experimental level. Chaotic sound makes clearer images of defects, but a pure 20-kHz frequency propagates further and, therefore, covers more area.

Sonic infrared (IR) is a viable technology, not only for cracks in metals, but also for delaminations and disbonds in composites. It is good at finding and sizing impact damage on aircraft composite skins and can also detect kissing disbonds that may be missed by thermal wave systems. With additional programming, the Sonic IR software could also determine defect depths. If used only for composites, Sonic IR does not require cameras with high frame rates.

Sonic IR is the fastest existing technology for wide-area inspection of composite structures as of this writing; images of areas as large as 12 square feet take only a few seconds to acquire and display. However, Sonic IR systems for composites should be restricted to relatively low power (i.e., only a few hundred watts) and use large-diameter ultrasonic horns to avoid risk of damage.

A mobile Sonic IR prototype system has been designed, constructed, and successfully tested on samples from Bell Helicopter and Boeing Commercial Airplanes. It is recommended that it now be tested on a composite fuselage with known internal damage.

APPENDIX A—PHOTOGRAPHS AND IMAGES OF SAMPLES

A.1. AIRBUS VERTICAL STABILIZER PANEL

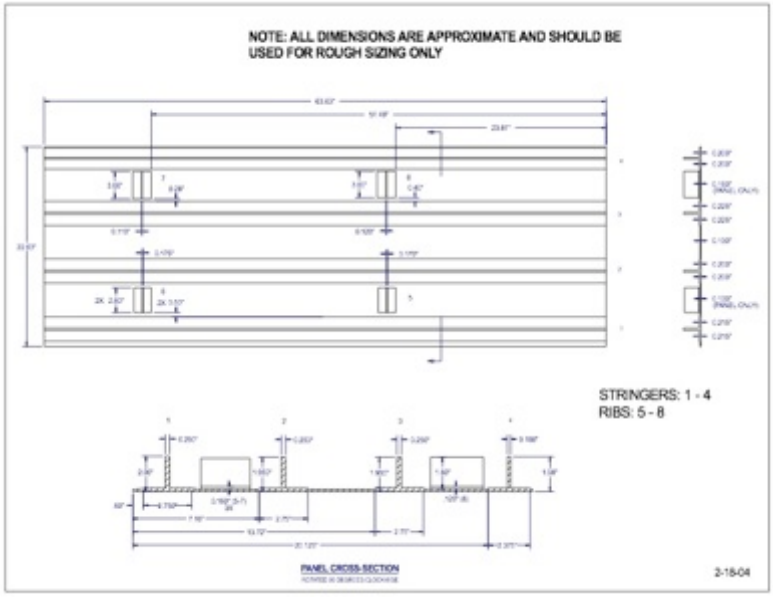

Figure A-1. Engineering drawing of the Airbus A-330 vertical stabilizer panel (the panel is 63.75″ x 22.50″ x 1.75″, including four enhancement ribs and four stiffeners on the backside of the panel)

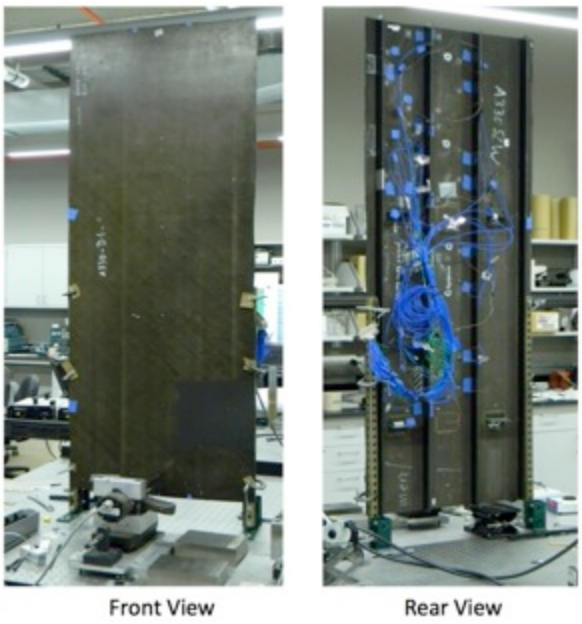

Figure A-2. Photographs of front and rear of the Airbus vertical stabilizer panel showing attached strain gauges and wiring

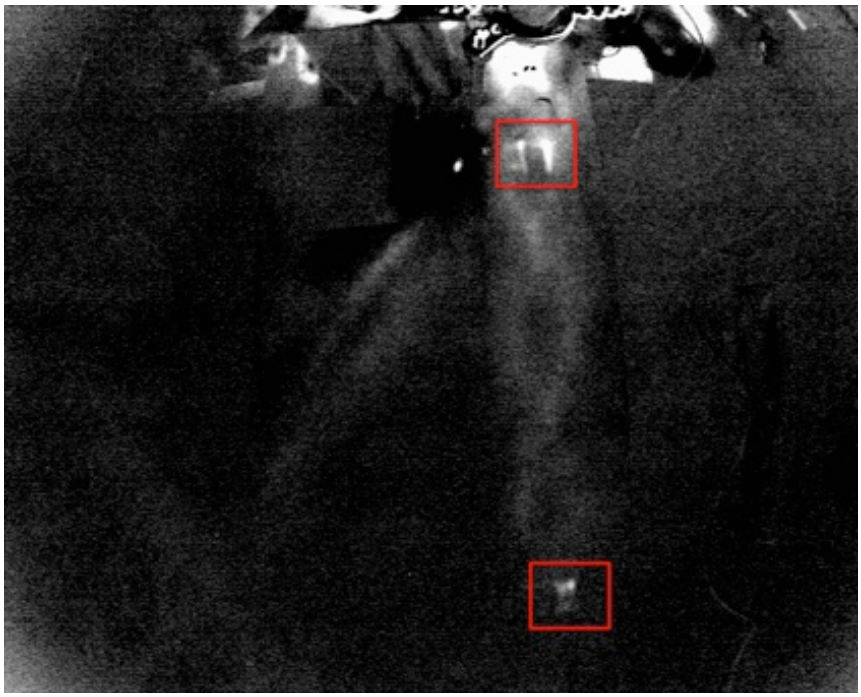

Figure A-3. Sonic IR image taken from the front side of the Airbus panel showing the kissing disbonds at two of the small stiffeners located on the rear side of the panel (the transducer was placed at the top end of the front of the panel. The image at the top of the panel is the reflection of the operator.)

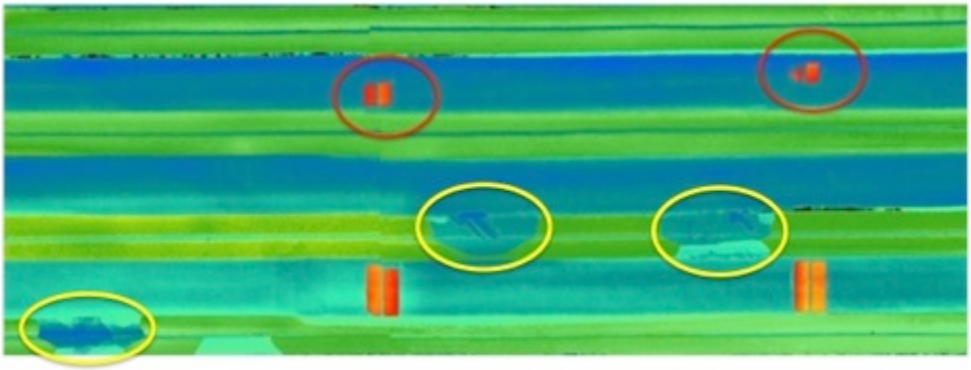

Figure A-4. Ultrasonic image of the Airbus panel (the red ovals indicate the positions of the two partially bonded [i.e., "kissing"] stiffeners seen in the Sonic IR image in figure A-3. The two stiffeners in the bottom channel are bonded in the ultrasonic image and, therefore, are not seen in Sonic IR images of the panel. The yellow ovals indicate fabricated stringer-to-skin separations that serve as additional ultrasonic targets. Only one of these appears in Sonic IR images [see figure 10, main report] because the fabricated gaps between the skin and the stringers in the others are too large to provide any contact and do not simulate real disbonds.)

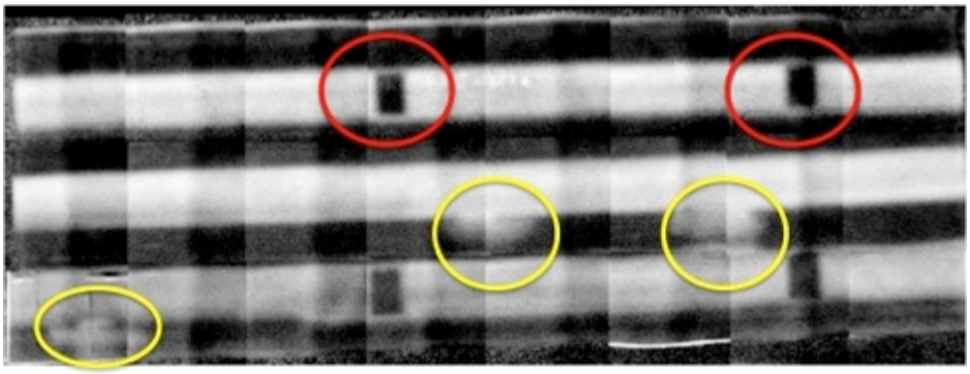

Figure A-5. Image of the Airbus panel made with a commercial thermal wave system (in this thermal wave image, bonded structures appear dark and unbonded ones light. The red ovals indicate the locations of the two partially bonded stiffeners that appear [incorrectly] to be bonded in this thermal wave image. It was images such as this that led to the "kissing disbond" designation for these two stiffeners. Note that the fabricated gaps between the stringers and the skin [indicated by yellow ovals] can be seen as disbonded. Also note that this image is actually a montage of 24 separate thermal wave images that must have taken considerable time to acquire and assemble. This is in contrast to the less than five seconds needed to acquire and display the Sonic IR image of this same panel in figure A-3 or figure 10 in the main report. The gray vertical stripes in the image apparently are an artifact of the process used to combine the 24 images, because they align with the right edge of each individual image.)

A.2 BELL HELICOPTER PANELS

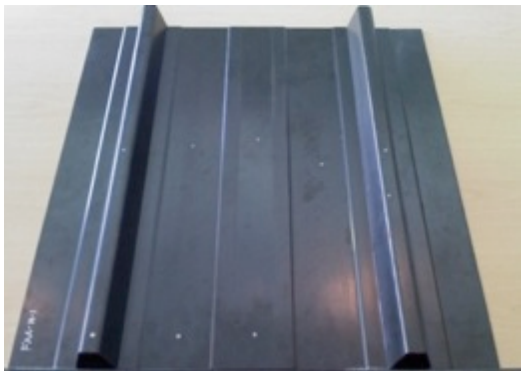

Figure A-6. Photograph of the rear side of the 2′ x 2′ hat channel panel from Bell Helicopter

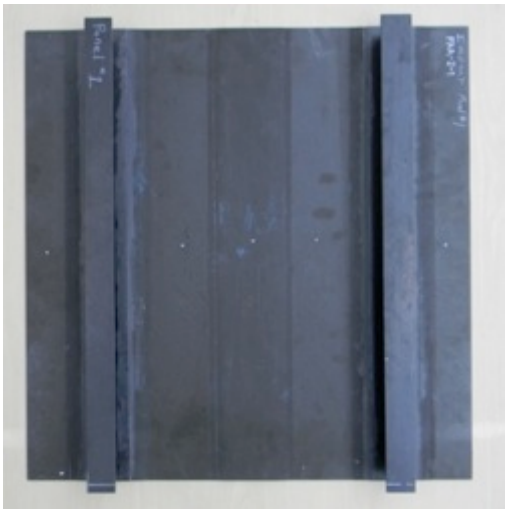

Figure A-7. Photograph of the rear side of the 2′ x 2′ I-beam panel from Bell Helicopter

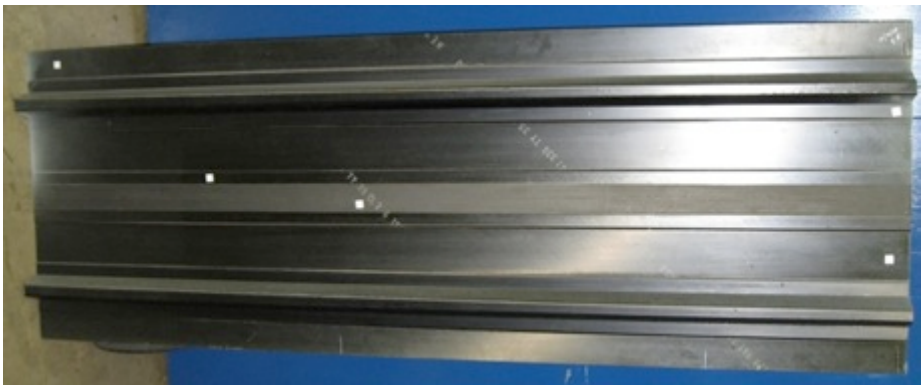

Figure A-8. Photograph of the larger hat channel panel from Bell Helicopter

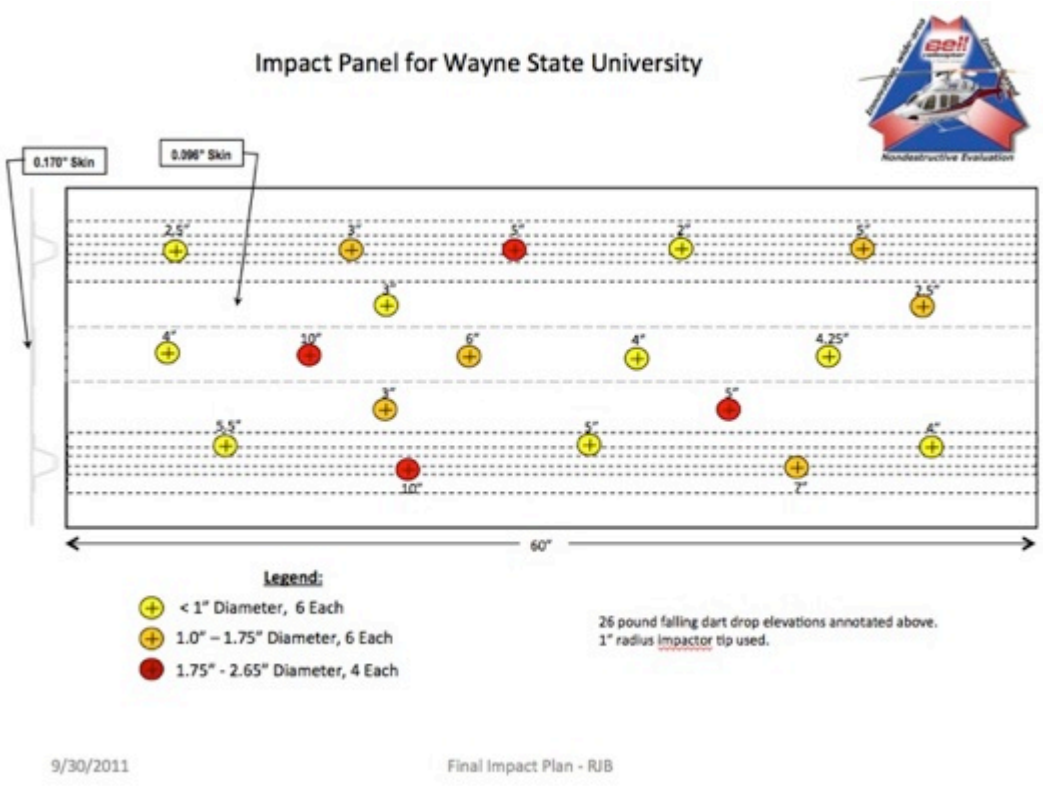

Figure A-9. Impact plan on the 22″ x 60″ hat panel (the intended defect locations are indicated in the drawing. In addition, the elevation values at which a 26-pound falling dart with a 1″ radius impactor tip was dropped are shown)

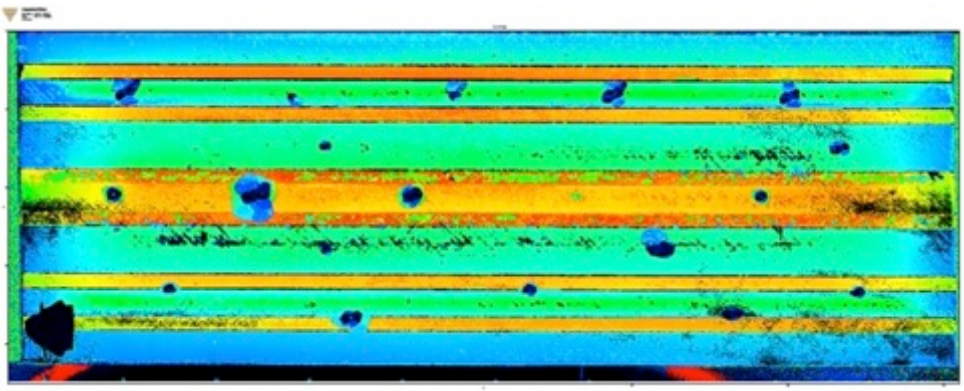

Figure A-10. Ultrasonic time-of-flight scan of the large hat channel sample (the panel is approximately 22″ x 60″)

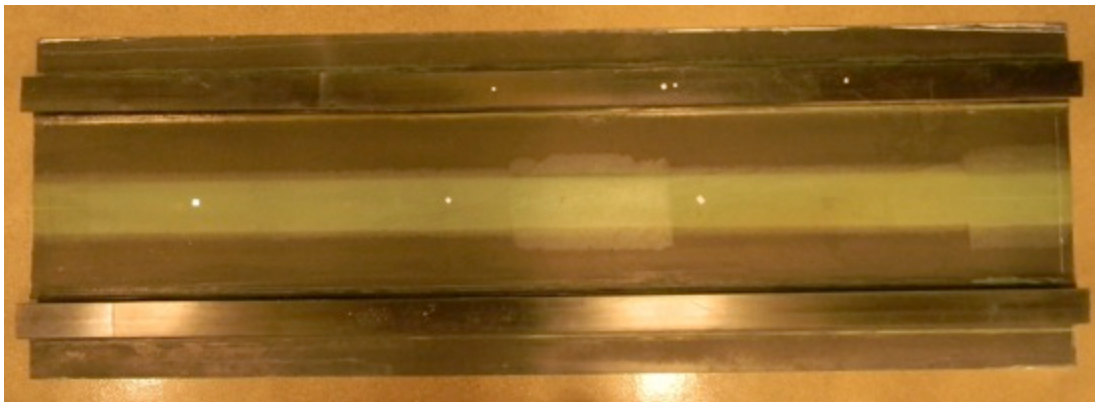

Figure A-11. Photograph of the larger I-beam channel panel from Bell Helicopter

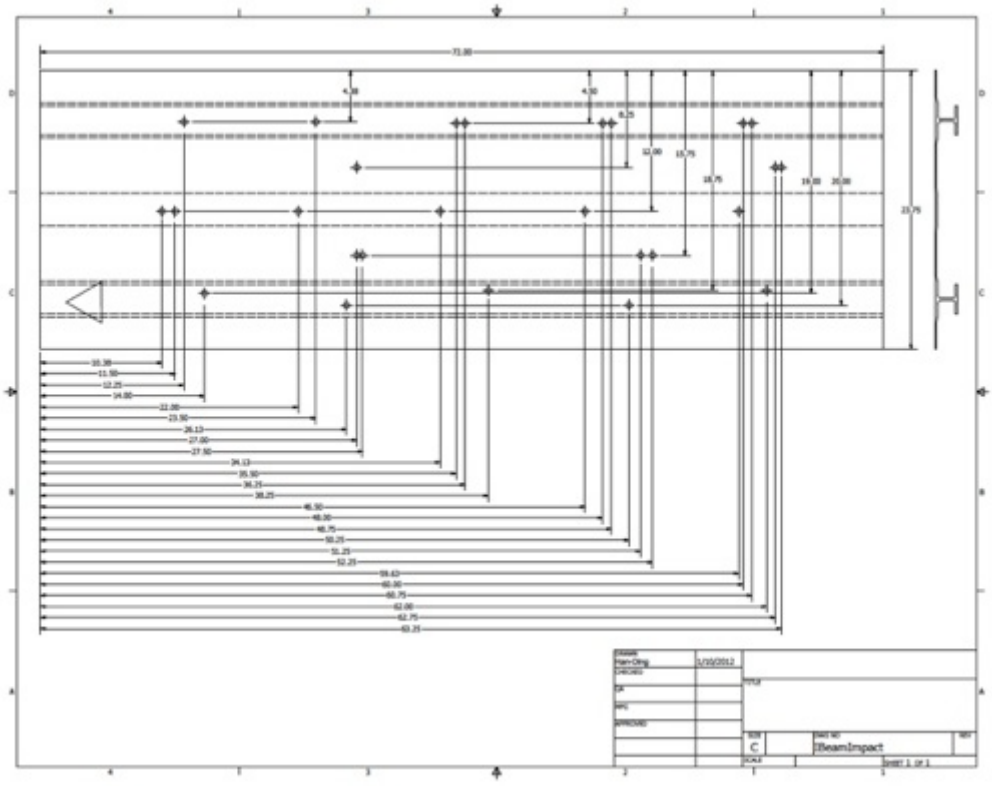

Figure A-12. Drawing of the 24″ x 72″ I-beam panel with locations of impacts as measured at Wayne State University

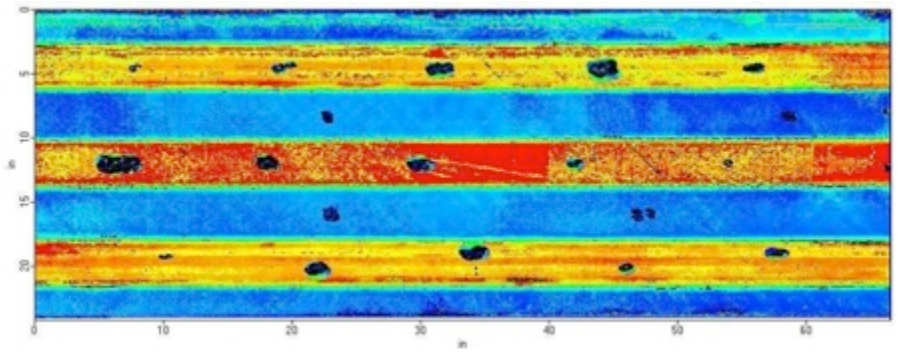

Figure A-13. Ultrasonic time-of-flight scan of the large I-beam sample (the panel is approximately 24″ x 72″)

A.3 THE FOUR PROTOTYPE EVALUATION TEAMS

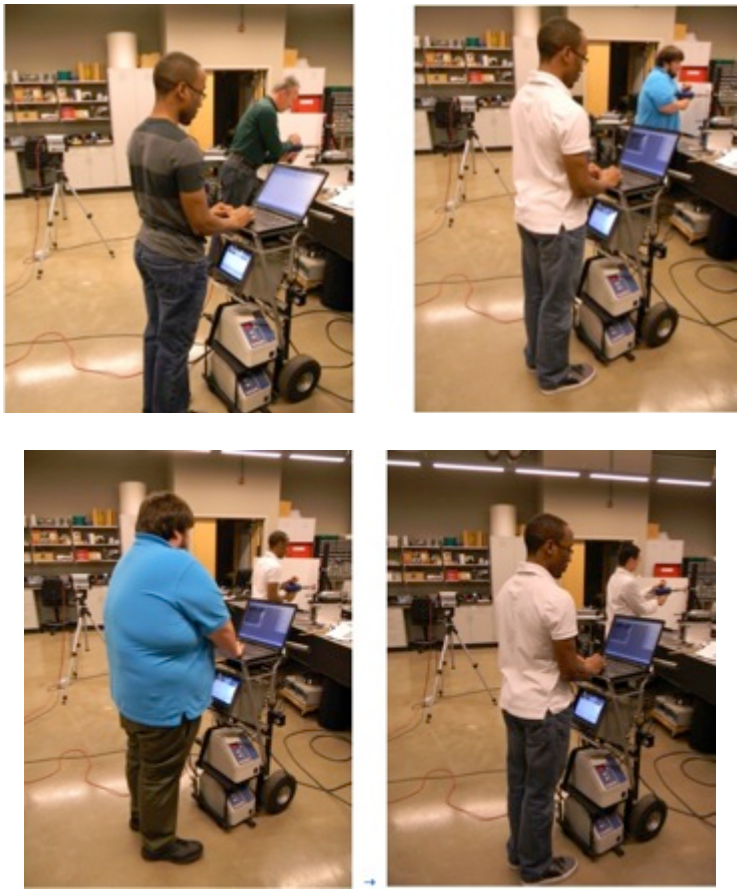

Figure A-14. Photographs of the four evaluation teams (the use of the word "team" here is perhaps somewhat misleading. Actually, it is only the person who is injecting the sound into the panel that has any ability to affect the result of the inspection. The person at the computer is merely clicking the mouse to trigger the software. The acquisition of the image is completely automatic after that click.)

APPENDIX B—EVALUATION OF OPERATOR DEPENDENCE

B.1 EVALUATION OF PROTOTYPE SYSTEM FOR OPERATOR DEPENDENCE

The statistical testing of the prototype for operator dependence was done with four 2-person teams. The use of the word "team" here is a bit misleading, because one member of the team (i.e., the person operating the computer) has no influence on the outcome. It was the person who was injecting the sound with the handheld transducer who determined the success or failure of each 0.8 second ultrasound sound pulse. In one such test, each operator repeated the imaging process five times, with the transducer at each end of the 6′ long Bell Helicopter sample shown in figure B-1, for a total of 10 distinct measurements made by each operator. After each pulse, the resulting Sonic IR image was evaluated for the visibility of damage at each of the 19 impact sites, which are labeled A to S in the ultrasonic image. This was done not only by visual inspection of the images, but also with temperature versus time plots for each of the sites to determine how much the signal from any Sonic IR damage indication rose above the background. The plotting routine was built into the Wayne State University software. An example of the use of this software on a typical image is shown in figure B-2. If this process resulted in a decision of "found," a "1" was placed in the corresponding cell in a table. If the decision was "not found," the cell was left blank. The raw data from this process for the Bell Helicopter I-beam sample can be found in appendix C.

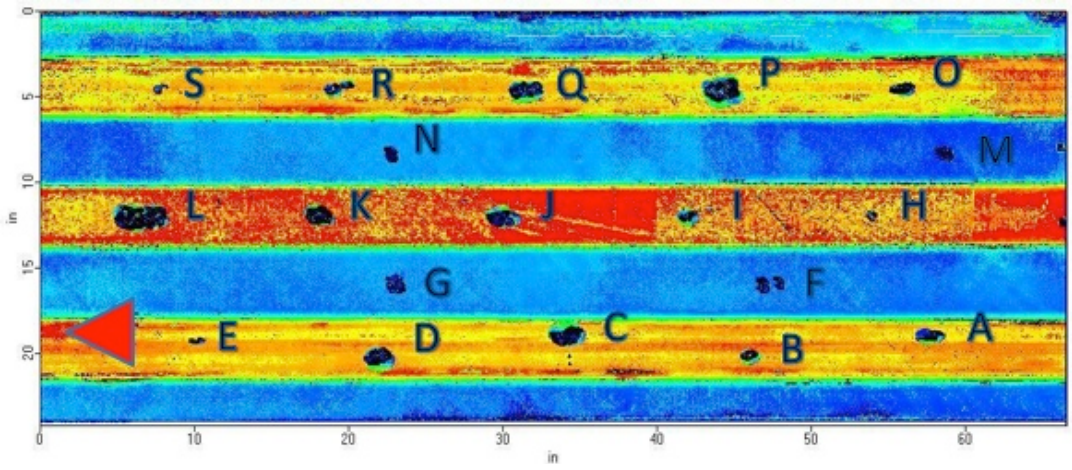

Figure B-1. Ultrasonic image of the 6′ long I-beam sample, with impact sites labeled A to S (the actual amount of damage at each site is unknown, but the size of an indication on this ultrasonic image gives some idea of the area damaged. The red triangle is the location of the Bell Helicopter label.)

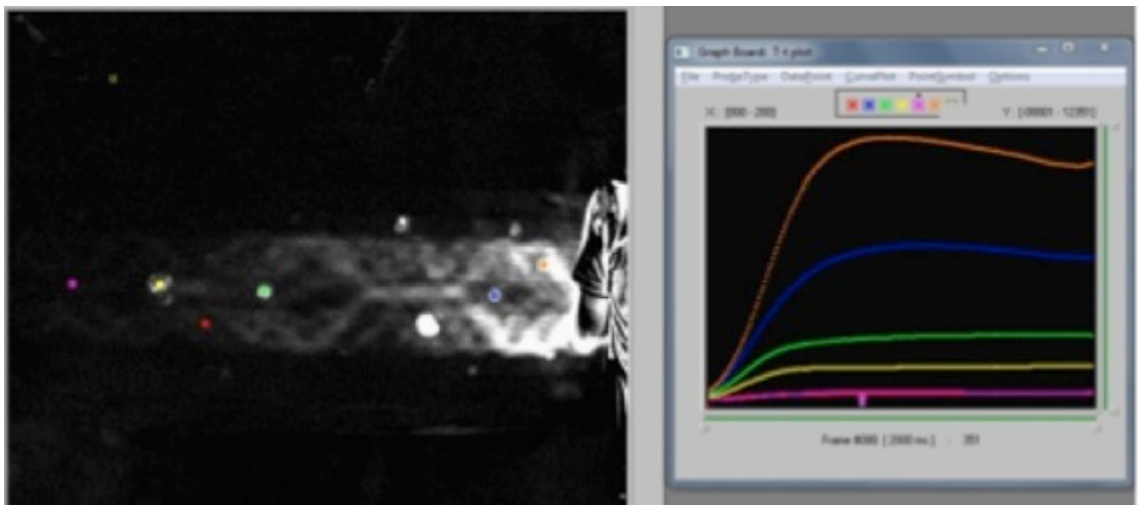

Figure B-2. An IR image showing the impact damage detected with the 20 kHz, 1-inch transducer held at the right side of the large hat beam panel by Operator I (six spots were chosen to show the temperature vs. time plots on those spots. The plotting window together with the image was captured from the screen of the prototype's computer.)

Table C-1 in appendix C contains 40 raw data entries organized as follows: the columns labeled A–S correspond to the labeled impact sites on the ultrasonic image in figure B-1. The first 10 data rows below the labels correspond to Operator I's results and include five from the right side of the panel followed by five from the left. The next 10 rows are for Operator II, followed by ten for Operator III and then ten for Operator IV. Operator I was a technician with the most experience; Operators III and IV were essentially beginners; and Operator II possessed an experience level between those levels. The last row at the bottom, just above the labels, is the sum of the results over all 40 trials for each impact site. This effectively shows the Sonic IR detectability of any damage at that particular site averaged over the four operators. Similarly, the numbers in the next to last column are the sums of the numbers of "finds" for each run of the system. Finally, the grand total of finds for each operator is shown in the last column. These range from 95–103 and can be considered a score for each operator. The differences in the numbers are probably not large enough to be statistically significant. The two most inexperienced operators (both were first year students) did get the two lowest scores, but the most experienced operator did not get the highest. The closeness of these scores and others like them in tests on both large Bell Helicopter samples seems to indicate that the results are not strongly affected by the experience of the operator.

The 40 inspections described above were set up for operator evaluations, not so that the maximum number of defects would be found. This was done by centering the transducer between the two stringers on the panel to maximize their waveguide effect on the sound. The horn on the transducer during these runs was 3/4″ in diameter, not the 1″ tip recommended for the final design of the prototype. This reduced its efficiency somewhat relative to the final system. The distance from the transducer to the defects was maximized by placing the transducer alternately on the extreme right or left front edges of the panel. This meant that the sound was injected over the ends of the central doubler on the back of the panel and that it propagated primarily down the channel between the stringers.

Nine impact sites were in the primary propagation zone, namely sites F–N. Of these sites, G, J, and N were seen in all 40 trials. Sites F, K, and L were each missed once. Site M was missed three times, but it is small and almost always partially obscured by the edge-effect interference pattern when sound is injected from the right side. Site I is very small, but was seen 18 times from the right. Site H, which is probably too small to be seen from the left, was missed; if a signal was present, it was obscured by the interference pattern from the right.

The sites outside the main propagation zone were wide ranging. Site C was seen every time, but it is quite large and on the edge of the zone. However, site A is also on the edge of the zone and was seen above the interference pattern only four times. Sites D and B are on the "wrong" side of the stringer, but D was seen 10 times and always from the left. Site E was never seen.

Sites O–S are all directly on the upper stringer. Of these, site P was missed only twice, and Q was seen nine times, all from the left. Sites O, R, and S were missed.

The patterns of found and missed sites above were consistent among the operators. Sites C, G, J, N, F, K, L, and P have a high probability of detection and were almost always found, regardless of who was operating the equipment. Site I was almost always found from the right, but never from the left. Sites D and Q were found approximately half the time, but only from the left. The rest were either outside the area that received enough sound, were obscured by interference patterns, or had so little damage that no heat from it ever reached the surface. However, all of the impact sites, except for S, were seen in other experiments that were set up differently from this specific operator evaluation arrangement.

APPENDIX C—RAW DATA FOR LARGE BELL I-BEAM SAMPLE
WITH FOUR OPERATORS

Table C-1: Raw data for large Bell I-beam sample with four operators

	A	B	C	D	E	F	G	H	I	J	K	L	M	N	O	P	Q	R	S		
Right I																					
1	1		1			1	1		1	1	1		1	1		1				10	
2	1		1			1	1		1	1	1	1	1	1		1				11	
3	1		1			1	1		1	1	1	1	1	1		1				11	
4			1			1	1			1	1	1	1	1		1				9	
5	1		1			1	1		1	1	1	1	1	1		1				11	
Left I																					98
1			1			1	1			1	1	1	1	1						8	
2			1			1	1			1	1	1	1	1		1				9	
3			1			1	1			1	1	1	1	1		1	1			10	
4			1			1	1			1	1	1	1	1		1				9	
5			1			1	1			1	1	1	1	1		1	1			10	
Right II																					
1			1			1	1		1	1	1	1	1	1		1				10	
2			1			1	1		1	1	1	1	1	1		1				10	
3			1			1	1		1	1	1	1	1	1		1				10	
4			1			1	1		1	1	1	1	1	1		1				10	
5			1			1	1		1	1	1	1	1	1		1				10	
Left II																					103
1			1			1	1			1	1	1	1	1		1				9	
2			1	1		1	1			1	1	1	1	1		1	1			11	
3			1	1		1	1			1	1	1	1	1		1	1			11	
4			1	1		1	1			1	1	1	1	1		1	1			11	
5			1	1		1	1			1	1	1	1	1		1	1			11	
Right III																					
1			1			1	1		1	1	1	1		1		1				9	
2			1			1	1		1	1	1	1	1	1		1				10	
3			1			1	1		1	1	1	1		1		1				9	
4			1			1	1		1	1		1	1	1		1				9	
5			1			1	1		1	1	1	1	1	1		1				10	
Left III																					97
1			1			1	1			1	1	1	1	1		1	1			10	
2			1			1	1			1	1	1	1	1		1	1			10	
3			1			1	1			1	1	1	1	1		1				9	
4			1	1		1	1			1	1	1	1	1		1				10	
5			1	1		1	1			1	1	1	1	1		1	1			11	
Right IV																					
1			1			1	1		1	1	1	1	1	1		1				10	
2			1			1	1		1	1	1	1	1	1		1				10	
3			1			1	1		1	1	1	1	1	1		1				10	
4			1			1	1			1	1	1	1	1		1				9	
5			1			1	1			1	1	1	1	1		1				9	

Table C-1: Raw data for large Bell I-beam sample with four operators (continued)

	A	B	C	D	E	F	G	H	I	J	K	L	M	N	O	P	Q	R	S		
Left IV																					95
1			1	1		1	1		1	1	1	1	1	1		1				11	
2			1	1		1	1			1	1	1	1	1						9	
3			1	1		1	1			1	1	1	1	1		1				10	
4			1			1	1			1	1	1	1	1		1				9	
5			1	1			1			1	1	1		1		1				8	
	4	0	40	10	0	39	40	0	18	40	39	39	37	40	0	38	9	0	0		
	A	B	C	D	E	F	G	H	I	J	K	L	M	N	O	P	Q	R	S		